Title

Controlling Dark Equilibria and Enhancing Donor–Acceptor Stenhouse Adduct Photoswitching Properties through Carbon Acid Design

Journal

Journal of the American Chemical Society, 140(33)

ISSN

0002-7863

Authors

Hemmer, James R
Page, Zachariah A
Clark, Kyle D
et al.

Publication Date

2018-08-22

DOI

10.1021/jacs.8b06067

Peer reviewed

JACS
JOURNAL OF THE AMERICAN CHEMICAL SOCIETY
Communication
Cite This: J. Am. Chem. Soc. XXXX, XXX, XXX−XXX
pubs.acs.org/JACS

Controlling Dark Equilibria and Enhancing Donor−Acceptor Stenhouse Adduct Photoswitching Properties through Carbon Acid Design

James R. Hemmer,[†] Zachariah A. Page,[‡] Kyle D. Clark,[†] Friedrich Stricker,[†] Neil D. Dolinski,[‡] Craig J. Hawker,[†,‡] and Javier Read de Alaniz*[,†]

[†]Department of Chemistry and Biochemistry, University of California−Santa Barbara, Santa Barbara, California 93106, United States

[‡]Materials Department, University of California−Santa Barbara, Santa Barbara, California 93106, United States

Supporting Information

ABSTRACT: A novel library of tunable negative photochromic compounds, donor−acceptor Stenhouse adducts (DASAs), is reported. Tailoring the electron deficient "acceptor" moiety yielded DASAs that can be activated with mild visible and far red light. The effect of acceptor composition on reactivity, absorption, equilibrium, and cyclability is exploited for the design of high performance photoswitches. The structural changes to the carbon acid acceptor also provide access to new, more structurally diverse DASA derivatives by facilitating the ring-opening reaction with electron deficient amine donors.

The ability to utilize light as a stimulus to induce molecular transformations has drawn significant attention, given that it can lead to unique property alterations in targeted applications that require spatial control. In particular, photoswitches have shown impressive changes to absorption, polarity, and geometry upon exposure to light, leading to desirable applications, such as cargo delivery,[1] sensing,[2] and actuation.[3] Consequently, an immense amount of research has gone into the development and optimization of photoswitch performance in order to harness their full potential in the medically relevant long-wavelength region (λ = 650−1450 nm).[4] Although photoswitch performance can be assessed through a number of parameters,[5] such as addressability, thermal stability, efficiency, and reliability, the ability to modulate photoswitchable systems with long-wavelength light is of central importance to all fields of life and materials science; ranging from the nascent fields of photopharmacology[6] to multiphotoresponsive molecular systems.[7] Additionally, the photoswitch should display quantitative conversion between its two isomers to maximize photoswitching performance.

Several decades of research have led to the development of a range of visible to far red light-driven photoswitches.[8] Of these, azobenzene is one of the fastest growing classes of photoswitches that respond to long-wavelength light.[9a,4a,9b−f] This growth can be attributed to a deeper understanding of the factors that influence the thermal half-life and the bathochromic shift of the excitation wavelength. More recently, indigoid photoswitches have shown great promise as long wavelength photoswitches, with facile synthesis and highly tunable absorption profiles, switching kinetics, and equilibria.[10] Although the utility of these systems is unquestionable, azobenzene- and indigoid-based photoswitches transition from one colored state to another, as opposed to cycling between colored and colorless states, which is often desirable to maximize light penetration and actuation power by driving photoisomerization volume changes throughout the depth of a material. Photochromic materials that lose absorption at the wavelength(s) of irradiation upon switching maximize light penetration. Negative photochromic material, which are capable of converting the thermodynamically favored colored isomer into an optically transparent colorless isomer upon exposure to light, are ideally positioned to achieve just that.[11] Donor−acceptor Stenhouse adducts (DASAs) are an emerging class of negative photochromic material (Figure 1a), containing a "donor" amine and a carbon acid "acceptor" linked through a triene-enol backbone.[12] Upon light irradiation, the triene undergoes a Z−E isomerization followed by a thermal 4π electrocyclization to yield a compact colorless cyclopentenone, which thermally reverts back to the extended linear colored isomer.[13] Combined, these features provide a means to enhance light penetration depth and actuation in bulk materials. Despite tremendous advances,[12] the development of DASA-based photoswitch materials that simultaneously controls the thermal equilibrum between the open and closed isomer and red-shift the excitation wavelength remains elusive.

The first generation DASAs contained secondary alkyl amine donors and either Meldrum's (**1**) or barbituric (**2**) acid acceptors.[14] Though these derivatives were favorably in the colored/triene state (>95%) at thermal equilibria in dichloromethane, they had a limited absorption window (λ = 545−570 nm) and were reversibly active in nonpolar media (e.g., toluene, hexanes, etc.). To address these limitations, second generation DASAs were developed by tuning the donor group using a range of aniline derivatives, while continuing to employ acceptors **1** and **2**.[7a,15] Though these modifications imparted improved color tunability and switchability in polar and nonpolar media, the thermodynamic equilibrium between the

Received: June 8, 2018
Published: August 3, 2018

DOI: 10.1021/jacs.8b06067
J. Am. Chem. Soc. XXXX, XXX, XXX−XXX

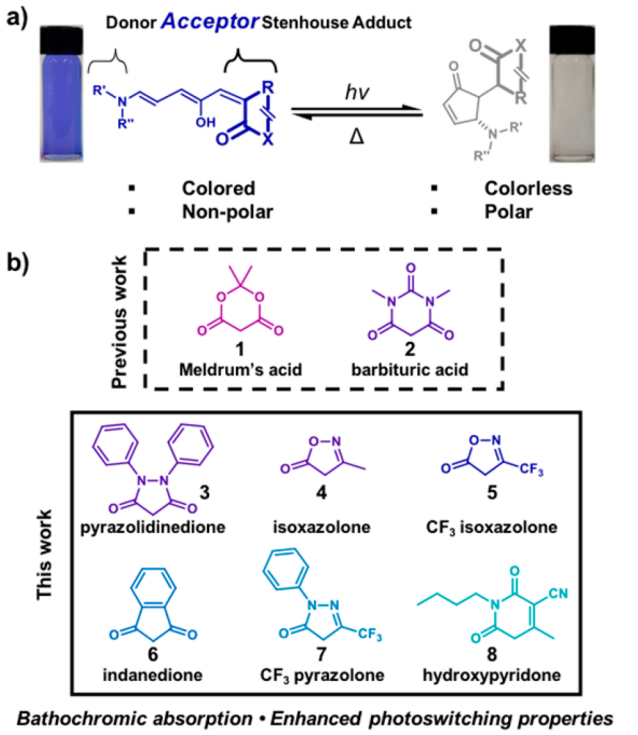

Figure 1. Donor–acceptor Stenhouse adducts (DASAs) (a) General structures for open/colored triene and closed/colorless cyclopentenone isomers. (b) Chemical structures for carbon acid acceptors examined previously (top) and novel structures from this report (bottom).

open and closed form was compromised, ranging from as low as 2% to 70% in the colored/triene state in the dark in dichloromethane.[16] For numerous applications, such as sensing and actuation, isomerization in the dark must be avoided in order to maximize the light-driven property changes.

Herein we report the facile synthesis of third generation DASAs where the carbon acid acceptor group is tailored to provide switching with far red light while simultaneously controlling the thermal equilibrium and thus enabling >95% conversion from the colored linear form to the colorless compact form upon exposure to light. Additionally, these new derivatives have increased synthetic diversity, wide color tunability (λ = 585–735 nm), and enhanced switching kinetics.

The six carbon acid acceptors utilized in this work were pyrazolidinedione (**3**), methyl isoxazolone (**4**), trfluoromethyl isoxazolone (**5**), indandione (**6**), trifluoromethyl pyrazolone (**7**), and hydroxypyridone (**8**), which were all synthesized in one pot from commercially available starting materials (see SI for more details) (Figure 1b). Knoevenagel condensation of the various carbon acids with furfural on water or neat (+ catalytic proline) provided the desired activated furan, which was susceptible to ring-opening by an amine donor to yield the corresponding DASA derivative (Scheme 1). The facile two-step procedure provides the desired compounds as solids that can be simply filtered and triturated for purification.

In all cases, the reaction between the amine donor and the activated furan proceeded as expected, but, impressively, the ring-opening reactions with the activated furan adduct of **5** were notably more exothermic than those observed with other furan adducts. When using diethylamine as the donor, the reaction with **5** was cooled to −78 °C to prevent side

Scheme 1. General DASA Synthesis[a]

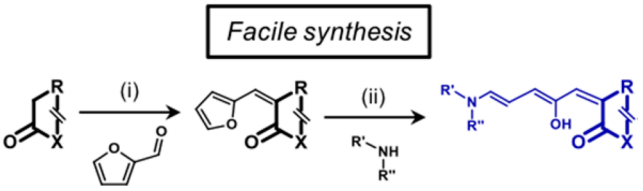

[a](i) water, or neat with proline, 30–89% yield; (ii) THF or methanol, 13–80% yield.

reactions, which suggested that the furan adduct of acceptor **5** had exceptional reactivity, likely due to the highly electron withdrawing nature of the carbon acid. To test this hypothesis, a weakly nucleophilic donor, bis(4-methoxyphenyl)amine, was mixed with the furan adduct of **1** (as a control) and **5** (Scheme 2). Though no reaction was observed using the previously

Scheme 2. Reactivity of p-OMe-Diphenylamine Donor with (a) Meldrum's Acid and (b) CF3 Isoxazolone Furan Adducts

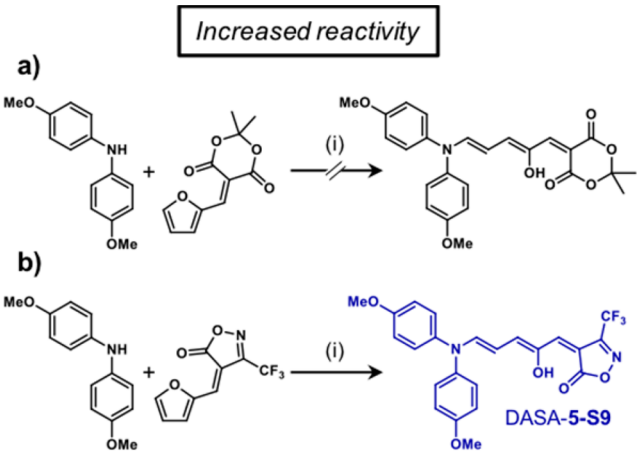

studied activated furan of **1**, the new furan adduct of **5** reacted at room temperature. The resulting DASA was photochromic, with an absorption maximum of ∼630 nm and near quantitative reversible switching (see SI for more details). This highlights how structural change in the carbon acid acceptors provide access to new, more structurally diverse DASA derivatives, with the potential for extended π-conjugation and bathochromic shift in absorption.

To compare the properties of the DASAs synthesized from these new carbon acid acceptors, diethylamine and 2-methylindoline were primarily used as the donor compounds. Analogous to our previous results, the indoline derivatives provide both a bathochromic shift in absorption and enhanced photoswitching properties relative to the diethylamine counterparts, and as such, will be the main subject of discussion, with complete details on all DASAs provided in the SI. The peak absorption ranged from 585 to 680 nm in going from acceptor **1** to **8** (Figure 2). Thus, the acceptor group was clearly shown to be a useful handle to tune the absorption of DASAs, with a marked improvement on the previously reported 15 nm difference observed between DASAs with acceptors **1** and **2**. Furthermore, the peak absorption could be extended to 690 and 735 nm by introducing an electron donating *para*-methoxy

DOI: 10.1021/jacs.8b06067
J. Am. Chem. Soc. XXXX, XXX, XXX–XXX

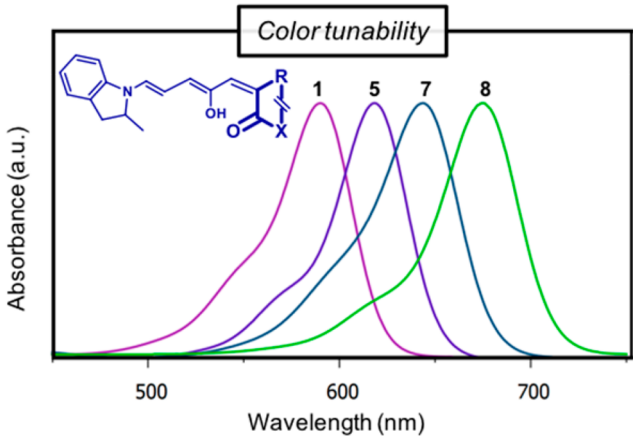

Figure 2. Absorption spectra for DASAs with a 2-methylindoline donor and various acceptors. Inset shows the general chemical structure and numbers refer to the acceptor group shown in Figure 1. See SI for comprehensive list of spectra.

or -diheptylamino substituent on the indoline moiety (Figure S4).

Having the ability to switch fully from one isomer to the other maximizes the change in properties, and as such, it is important to characterize the thermodynamic equilibrium for new photoswitches. For DASAs, it is desirable for the thermal equilibrium to favor (>95%) the triene isomer (colored form), with a complete transformation to the photostationary cyclopentenone isomer (colorless form) upon exposure to visible light. An attractive feature of negative photoswitches, like DASAs, is the improved light penetration upon excitation, which assists in driving the transformation to a >95% photostationary state (<5% triene). To determine the effect of acceptor composition on equilibrium position, the photoswitches were examined using[1] nuclear magnetic resonance (NMR) spectroscopy. Specifically, peaks at ∼11.6 and ∼6.3 ppm, which correspond to the alcohol proton and one of the triene protons, respectively, and ∼7.8 and ∼6.4 ppm, which correspond to protons on the cyclopentenone ring, were monitored in the absence of light until equilibrium was reached (Figure 3a). Compared to previously studied acceptors **1** and **2** (∼45% triene at equilibrium), all new acceptor groups, apart from **6**, favored the triene (colored form) relative to the cyclopentenone (colorless form) at equilibrium in chloroform (Figure 3b) (i.e., the new carbon acceptors shifted the equilbria toward the colored form). In particular, DASAs with acceptors **3**, **4**, and **8** were found to have triene equilibria ranging from ∼75−85%, whereas **5** and **7** were >95% in the triene form. Interestingly, when comparing methyl isoxazolone (**4**) to the more electron deficient trifluoromethyl isoxazolone (**5**) acceptor, there is a 20% shift in triene equilibrium, from 80 to >95%, respectively. Although it is not fully understood at this time, it is speculated that factors such as the acidity and orbital energy levels of the acceptors may play a role in dictating the equilibrium position for these DASA libraries.

In addition to the importance of maximizing the change in properties upon switching by tuning the equilibrium position, it is also essential to modulate the rate at which the photoisomerization reaction occurs, with rapid switching between the two states being desirable. To this end, DASA with acceptor **7** was examined in more detail, given its beneficial optical properties (λ_{max} ≈ 650 nm, > 95% triene at equilibrium). When comparing to previous DASAs, bearing

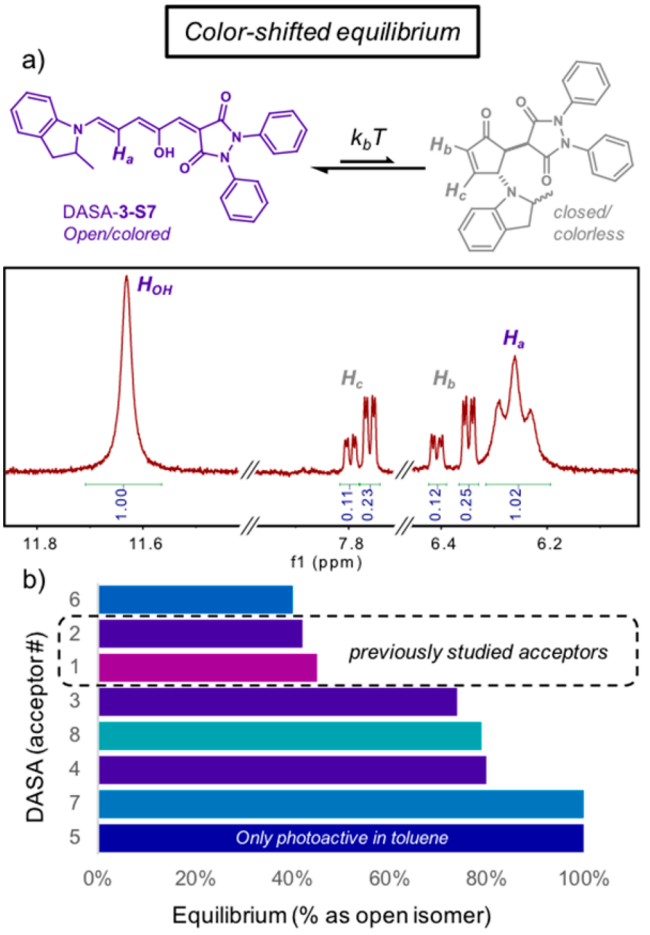

Figure 3. Equilibrium position for DASAs with a 2-methylindoline donor and indicated acceptors. (a) Representative DASA with acceptor 3 and corresponding ^{1}H NMR spectrum (see SI for full spectra). (b) Equilibrium position for DASAs with acceptors 1−8. Note: the ^{1}H NMR of the closed form results in a mixture of diastereomers.

either acceptor **1** or **2**, the switching upon exposure to visible light was found to be similar (∼5 s), yet the rate of thermal equilibration was impressively different. The DASA with acceptor **7** reverted back to the colored form within 60 s in the dark, whereas with acceptors **1** and **2** it took ∼8 and ∼2.5 h, respectively (Figures 4, S5, and S7). Furthermore, DASA with **7** reverted back to >95% triene, whereas DASA with **2** equilibrates to a ratio containing 50% of the triene. This stark difference highlights how the acceptor composition can be tailored to alter the switching kinetics of DASAs.

Given the less destructive and less harmful nature of long-wavelength light toward polymeric materials and biological cells, the ability to activate DASAs with 700 nm light was examined. The DASA with acceptor **8** was chosen since it provided the most red-shifted absorption ($CDCl_3$ λ_{max} = 680 nm with tail out to λ = 720 nm), and a far red light emitting diode (LED, λ_{ex} ≈ 700 nm) was used as the excitation source. In nonpolar solutions, this DASA derivative was shown to respond quickly to this light (<30 s), but in pure toluene had notable fatigue (∼70%/cycle; Figure S24). Introducing octane as a cosolvent was found to greatly improve fatigue resistance, which may be due to a reduced stability of the cyclopentenone isomer in less polar media. However, further improvements in stability during switching cycles is currently under examination.

DOI: 10.1021/jacs.8b06067
J. Am. Chem. Soc. XXXX, XXX, XXX−XXX

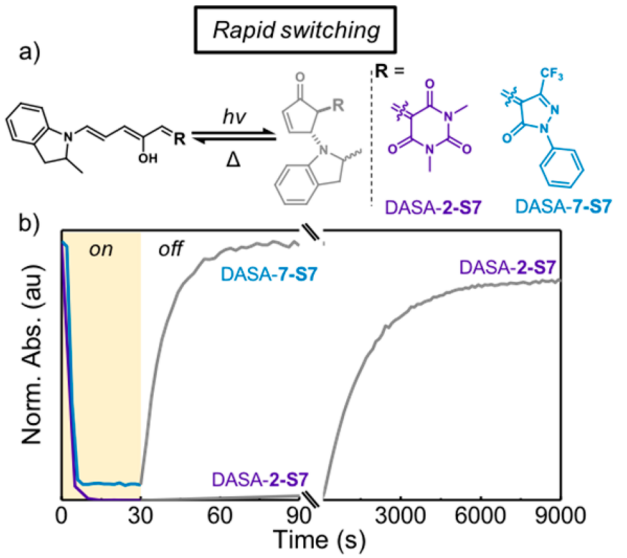

Figure 4. Increased DASA switching rate. (a) Chemical structure for DASA containing 2-methylindoline as the donor and acceptor 2 (top) and 7 (bottom). (b) Kinetics tracking the absorption maximum over time. Experiments performed under ambient conditions in $CDCl_3$.

Figure 5 shows 10 cycles of far red irradiation for DASA with acceptor **8** in a 3:1 mixture of toluene:octane. The DASA with

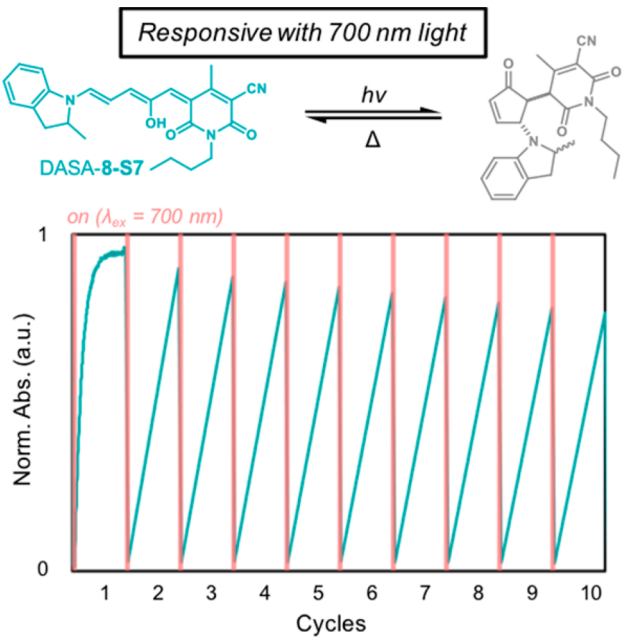

Figure 5. Fatigue resistance study was conducted under ambient conditions open to air using a 3:1 mixture of toluene:octane.

acceptor **8** reverted back to the colored form 5-times and 16-times faster than DASA with acceptors **1** and **2**, respectively. Beyond the enhanced switching properties, this is the first demonstration of a DASA photoswitch operating with 700 nm light and represents a rare example of a photoswitch that responds in the biologically important far red region (> 700 nm).[9e,17]

In summary, electron deficient acceptors in donor–acceptor Stenhouse adducts are excellent handles to tune the properties of this emerging class of photoswitch. Sixteen different third generation DASA derivatives were efficiently synthesized and characterized for their photochromic behavior. Improved reactivity, color tunability, thermodynamic equilibria, switching kinetics, and activity to far red light were observed when compared to previous generations. These improvements will guide the rational design of future DASA photoswitches, with potential applications as actuators for renewable energy and wavelength-selective delivery vehicles for medicine.[18]

■ ASSOCIATED CONTENT

Supporting Information

The Supporting Information is available free of charge on the ACS Publications website at DOI: 10.1021/jacs.8b06067.

Synthetic procedures, experimental details, and photophysical properties (PDF)

■ AUTHOR INFORMATION

Corresponding Author

*javier@chem.ucsb.edu

ORCID

Zachariah A. Page: 0000-0002-1013-5422

Craig J. Hawker: 0000-0001-9951-851X

Javier Read de Alaniz: 0000-0003-2770-9477

Notes

The authors declare no competing financial interest.

■ ACKNOWLEDGMENTS

C.J.H. and J.R.A. acknowledge that the research reported here made use of shared facilities of the UCSB MRSEC (NSF DMR 172056), a member of the Materials Reserarch Facilities Network (http://www.mrfn.org). We thank California Nano-Systems Institute (CNSI) Challenge Grant Program for support and Dr. Alexander Mikhailovsky for his help constructing the optical setup used for the switching experiments.

■ REFERENCES

(1) For select examples, see: (a) Tong, R.; Hemmati, H. D.; Langer, R.; Kohane, D. S. *J. Am. Chem. Soc.* **2012**, *134*, 8848–8855. (b) Goulet-Hanssens, A.; Barrett, C. J. *J. Polym. Sci., Part A: Polym. Chem.* **2013**, *51*, 3058–3070. (c) Poelma, S. O.; Oh, S. S.; Helmy, S.; Knight, A. S.; Burnett, G. L.; Soh, H. T.; Hawker, C. J.; Read de Alaniz, J. *Chem. Commun.* **2016**, *52*, 10525–10528.

(2) For select examples, see: (a) Nam, Y.-S.; Yoo, I.; Yarimaga, O.; Park, I. S.; Park, D.-H.; Song, S.; Kim, J.-M.; Lee, C. W. *Chem. Commun.* **2014**, *50*, 4251–4254. (b) Tatum, L. A.; Su, X.; Aprahamian, I. *Acc. Chem. Res.* **2014**, *47*, 2141–2149. (c) Balamurugan, A.; Lee, H.-i. *Macromolecules* **2016**, *49*, 2568–2574. (d) Diaz, Y. J.; Page, Z. A.; Knight, A. S.; Treat, N. J.; Hemmer, J. R.; Hawker, C. J.; Read de Alaniz, J. *Chem. - Eur. J.* **2017**, *23*, 3562–3566.

(3) *Photomechanical Materials, Composites, and Systems*; White, T. J., Ed.; John Wiley & Sons, Ltd, 2017; pp 1–416.

(4) For select reviews, see: (a) Bandara, H. M. D.; Burdette, S. C. *Chem. Soc. Rev.* **2012**, *41*, 1809–1825. (b) Irie, M.; Fukaminato, T.; Matsuda, K.; Kobatake, S. *Chem. Rev.* **2014**, *114*, 12174–12277. (c) Klajn, R. *Chem. Soc. Rev.* **2014**, *43*, 148–184.

(5) van Dijken, D. J.; Kovaříček, P.; Ihrig, S. P.; Hecht, S. *J. Am. Chem. Soc.* **2015**, *137*, 14982–14991.

(6) For select examples, see: (a) Velema, W. A.; Szymanski, W.; Feringa, B. L. *J. Am. Chem. Soc.* **2014**, *136*, 2178–2191. (b) Broichhagen, J.; Frank, J. A.; Trauner, D. *Acc. Chem. Res.* **2015**, *48*, 1947–1960. (c) Lerch, M. M.; Hansen, M. J.; van Dam, G. M.; Szymanski, W.; Feringa, B. L. *Angew. Chem., Int. Ed.* **2016**, *55*, 10978–10999.

DOI: 10.1021/jacs.8b06067
J. Am. Chem. Soc. XXXX, XXX, XXX–XXX

(7) (a) Hemmer, J. R.; Poelma, S. O.; Treat, N.; Page, Z. A.; Dolinski, N.; Diaz, Y. J.; Tomlinson, W.; Clark, K. D.; Hooper, J. P.; Hawker, C. J.; Read de Alaniz, J. *J. Am. Chem. Soc.* **2016**, *138*, 13960. (b) Lerch, M. M.; Hansen, M. J.; Velema, W. A.; Szymanski, W.; Feringa, B. L. *Nat. Commun.* **2016**, *7*, 12054. (c) Ulrich, S.; Hemmer, J. R.; Page, Z. A.; Dolinski, N. D.; Rifaie-Graham, O.; Bruns, N.; Hawker, C. J.; Boesel, L. F.; Read de Alaniz, J. *ACS Macro Lett.* **2017**, *6*, 738−742.

(8) For select examples, see: (a) Patel, D. G.; Paquette, M. M.; Kopelman, R. A.; Kaminsky, W.; Ferguson, M. J.; Frank, N. L. *J. Am. Chem. Soc.* **2010**, *132*, 12568−12586. (b) Hatano, S.; Horino, T.; Tokita, A.; Oshima, T.; Abe, J. *J. Am. Chem. Soc.* **2013**, *135*, 3164−3172. (c) Bleger, D.; Hecht, S. *Angew. Chem., Int. Ed.* **2015**, *54*, 11338−11349. (d) Calbo, J.; Weston, C. E.; White, A. J. P.; Rzepa, H. S.; Contreras-García, J.; Fuchter, M. J. *J. Am. Chem. Soc.* **2017**, *139*, 1261−1274. (e) Wilson, D.; Li, J. W.; Branda, N. R. *ChemMedChem* **2017**, *12*, 284−287. (f) van Leeuwen, T.; Pol, J.; Roke, D.; Wezenberg, S. J.; Feringa, B. L. *Org. Lett.* **2017**, *19*, 1402−1405.

(9) For select examples, see: (a) Beharry, A. A.; Sadovski, O.; Woolley, G. A. *J. Am. Chem. Soc.* **2011**, *133*, 19684−19687. (b) Bléger, D.; Schwarz, J.; Brouwer, A. M.; Hecht, S. *J. Am. Chem. Soc.* **2012**, *134*, 20597−20600. (c) Samanta, S.; Babalhavaeji, A.; Dong, M.-x.; Woolley, G. A. *Angew. Chem., Int. Ed.* **2013**, *52*, 14127−14130. (d) Knie, C.; Utecht, M.; Zhao, F.; Kulla, H.; Kovalenko, S.; Brouwer, A. M.; Saalfrank, P.; Hecht, S.; Bléger, D. *Chem. - Eur. J.* **2014**, *20*, 16492−16501. (e) Yang, Y.; Hughes, R. P.; Aprahamian, I. *J. Am. Chem. Soc.* **2014**, *136*, 13190−13193. (f) Hammerich, M.; Schütt, C.; Stähler, C.; Lentes, P.; Röhricht, F.; Höppner, R.; Herges, R. *J. Am. Chem. Soc.* **2016**, *138*, 13111−13114.

(10) (a) Kink, F.; Collado, M. P.; Wiedbrauk, S.; Mayer, P.; Dube, H. *Chem. - Eur. J.* **2017**, *23*, 6237−6243. (b) Huang, C.-Y.; Bonasera, A.; Hristov, L.; Garmshausen, Y.; Schmidt, B. M.; Jacquemin, D.; Hecht, S. *J. Am. Chem. Soc.* **2017**, *139*, 15205−15211. (c) Petermayer, C.; Thumser, S.; Kink, F.; Mayer, P.; Dube, H. *J. Am. Chem. Soc.* **2017**, *139*, 15060−15067. (d) Zweig, J. E.; Newhouse, T. R. *J. Am. Chem. Soc.* **2017**, *139*, 10956−10959. (e) Petermayer, C.; Dube, H. *Acc. Chem. Res.* **2018**, *51*, 1153−1163.

(11) Aiken, S.; Edgar, R. J. L.; Gabbutt, C. D.; Heron, B. M.; Hobson, P. A. *Dyes Pigm.* **2018**, *149*, 92−121.

(12) Lerch, M. M.; Szymanski, W.; Feringa, B. L. *Chem. Soc. Rev.* **2018**, *47*, 1910.

(13) (a) Lerch, M. M.; Wezenberg, S. J.; Szymanski, W.; Feringa, B. L. *J. Am. Chem. Soc.* **2016**, *138*, 6344−6347. (b) Di Donato, M.; Lerch, M. M.; Lapini, A.; Laurent, A. D.; Iagatti, A.; Bussotti, L.; Ihrig, S. P.; Medved, M.; Jacquemin, D.; Szymanski, W.; Buma, W. J.; Foggi, P.; Feringa, B. L. *J. Am. Chem. Soc.* **2017**, *139*, 15596−15599. (c) Lerch, M. M.; Medved, M.; Lapini, A.; Laurent, A. D.; Iagatti, A.; Bussotti, L.; Szymanski, W.; Buma, W. J.; Foggi, P.; Di Donato, M.; Feringa, B. L. *J. Phys. Chem. A* **2018**, *122*, 955−964.

(14) Helmy, S.; Leibfarth, F. A.; Oh, S.; Poelma, J. E.; Hawker, C. J.; Read de Alaniz, J. *J. Am. Chem. Soc.* **2014**, *136*, 8169−8172.

(15) Mallo, N.; Brown, P. T.; Iranmanesh, H.; MacDonald, T. S.; Teusner, M. J.; Harper, J. B.; Ball, G. E.; Beves, J. E. *Chem. Commun.* **2016**, *52*, 13576−13579.

(16) These ratios are for the dark equilibria (% open colored form) in CD_2Cl_2 with Meldrum's acid acceptor. Note, the dark equilibria vary depending on solvent and donor and/or acceptor group attached to DASA. See reference 12 for examples in various conditions.

(17) (a) Dong, M.; Babalhavaeji, A.; Collins, C. V.; Jarrah, K.; Sadovski, O.; Dai, Q.; Woolley, G. A. *J. Am. Chem. Soc.* **2017**, *139*, 13483−13486. (b) Klaue, K.; Garmshausen, Y.; Hecht, S. *Angew. Chem., Int. Ed.* **2018**, *57*, 1414−1417.

(18) Rifaie-Graham, O.; Ulrich, S.; Galensowske, N. F. B.; Balog, S.; Chami, M.; Rentsch, D.; Hemmer, J. R.; Read de Alaniz, J.; Boesel, L. F.; Bruns, N. *J. Am. Chem. Soc.* **2018**, *140*, 8027−8036.

DOI: 10.1021/jacs.8b06067
J. Am. Chem. Soc. XXXX, XXX, XXX−XXX